Redundant information encoding in QED during decoherence

J. Tuziemski,[1,2] P. Witas,[3] and J. K. Korbicz[1,2,*]

[1]*Faculty of Applied Physics and Mathematics, Gdańsk University of Technology, 80-233 Gdańsk, Poland*

[2]*National Quantum Information Centre in Gdańsk, 81-824 Sopot, Poland*

[3]*Institute of Physics, Faculty of Physics, Astronomy and Informatics Nicolaus Copernicus University, 87-100 Toruń, Poland*

(Received 12 October 2017; published 12 January 2018)

Broadly understood decoherence processes in quantum electrodynamics, induced by neglecting either the radiation [L. Landau, Z. Phys. **45**, 430 (1927)] or the charged matter [N. Bohr and L. Rosenfeld, K. Danske Vidensk. Selsk, Math.-Fys. Medd. **XII**, 8 (1933)], have been studied from the dawn of the theory. However, what happens in between, when a part of the radiation may be observed, as is the case in many real-life situations, has not been analyzed yet. We present such an analysis for a nonrelativistic, pointlike charge and thermal radiation. In the dipole approximation, we solve the dynamics and show that there is a regime where, despite the noise, the observed field carries away almost perfect and hugely redundant information about the charge momentum. We analyze a partial charge-field state and show that it approaches a so-called spectrum broadcast structure.

DOI: 10.1103/PhysRevA.97.012110

I. INTRODUCTION

The quantum information theory approach to open quantum systems has been the subject of active research recently, with the advent of such new and exciting research areas as thermodynamics of meso- and nanoscale systems [1–3] and quantum Darwinism [4–6], to name just two. Here we consider quantum electrodynamics (QED) from an open system's perspective (see [7–12] and the references therein), treating the electromagnetic field as the environment for the charge. We use quantum information concepts to study information gained by portions of the (initially thermal) field about the charge during the evolution. Consequently, we have to go beyond the usual approach to open systems, where the environment is assumed to pass unobserved and hence is traced out, and only the reduced state of the system is explicitly studied (see, e.g., [5,9]). This leads, under appropriate conditions, to the well-known phenomenon of decoherence, i.e., the loss of coherence in some preferred basis of the system, called the pointer basis. This phenomenon has been experimentally observed in a variety of systems [13]. In QED, decoherence due to various effects has been extensively studied (see, e.g., [10] for a review), including decoherence due to the dressing (e.g., in [12]), nonzero temperature [12], bremsstrahlung [9,11], and the charge monitoring the field [10].

Here instead, we assume that a part of the field is monitored and thus cannot be traced out. This line of thinking was introduced in the quantum Darwinism program [4–6] and further developed in the so-called spectrum broadcast structure approach to objectivity [14–17] (see also [18]). In the spirit of the latter, we study a partially traced state, containing a part of the radiation modes. We show that, under appropriate conditions and a certain coarse graining, almost perfect information about the charge momentum is encoded during the decoherence into the thermal field with a huge redundancy. It can be in principle extracted via projective measurements on the field modes with negligible disturbance to the partial charge-field state. This result is achieved via showing that the partially traced state approaches the so-called spectrum broadcast structure (SBS) [14–17]—a state structure describing broadcasting of the same classical information into multiple quantum systems. Some preliminary results along these lines were obtained in [12], where a buildup of correlations between momentum components of the charge and the dressing cloud was shown during the vacuum-induced decoherence. But neither the structure of the partially traced state has been considered nor the redundancy of information shown. Also, we show the redundant information transfer for the thermal, rather than for the vacuum field, which is more realistic and surprising due to the inherent noise.

We consider the nonrelativistic regime of QED and neglect any possible inner degrees of freedom of the charge, treating it as a free, pointlike particle of mass m_0 and charge q, interacting with an initially thermal field. The charge-field system is then described by the minimally coupled Hamiltonian with a necessary cutoff frequency $\bar{\Omega}$ to avoid the ultraviolet divergences,

$$\hat{H} = \frac{1}{2m_0}[\hat{\mathbf{p}} - q\hat{\mathbf{A}}(\hat{\mathbf{r}})]^2 + \sum_{\mathbf{k},j} \hbar\omega_{\mathbf{k}} \hat{a}^\dagger_{\mathbf{k},j}\hat{a}_{\mathbf{k},j}, \tag{1}$$

where the potential $\mathbf{A}(\mathbf{r})$ is chosen in the Coulomb gauge:

$$\hat{\mathbf{A}}(\hat{\mathbf{r}}) = \sum_{\mathbf{k},j} \boldsymbol{\epsilon}_{\mathbf{k},j} \sqrt{\frac{\hbar}{2\varepsilon_0\omega_{\mathbf{k}}V}} (\hat{a}^\dagger_{\mathbf{k},j} e^{-i\mathbf{k}\cdot\hat{\mathbf{r}}} + \hat{a}_{\mathbf{k},j} e^{\mathbf{k}\cdot\hat{\mathbf{r}}}). \tag{2}$$

Here $\boldsymbol{\epsilon}_{\mathbf{k},j}$ is the polarization vector of the mode $\mathbf{k}$, $\omega_{\mathbf{k}}$ is its frequency, the field is quantized in a box of volume V with the sum restricted to $\omega_{\mathbf{k}} \lesssim \bar{\Omega}$, and $\hat{a}_{\mathbf{k},j}$ and $\hat{a}^\dagger_{\mathbf{k},j}$ are the creation and annihilation operators obeying $[\hat{a}_{\mathbf{k},j}, \hat{a}^\dagger_{\mathbf{k}',j'}] = \delta_{\mathbf{k},\mathbf{k}'}\delta_{j,j'}$. We consider the charge initially described by a wave

*jkorbicz@mif.pg.gda.pl

packet localized at δr_0, small with respect to the shortest relevant wavelength of the field, and the cutoff is assumed to reflect this. The spreading limits the use in such cases of the usual dipole approximation (see, e.g., [19]) to times not much larger than $\bar{\Omega}^{-1}$. To somewhat improve the situation, we use the so-called moving dipole approximation, introduced in [12] and giving longer times. One follows with the dipole approximation the average packet position, assumed to travel along the free trajectory $\mathbf{r}(t) = \mathbf{r}_0 + \mathbf{v}_0 t$, with $\mathbf{v}_0$ the initial average particle velocity. The approximation breaks down when the packet width becomes comparable with $c/\bar{\Omega}$, which happens for

$$t \lesssim \tau_{\mathrm{dip}} \equiv \frac{m_0 c}{\bar{\Omega}\delta p_0}, \tag{3}$$

obtained assuming a minimal initial packet and free (i.e., non-interacting) spreading. The consistency of this approximation has been proven in [12]. Due to Eq. (3), the information accumulation effects require, as we will see, very strong coupling but, nevertheless, are in principle possible. Since we are interested in moderate field intensities we neglect the $\hat{\mathbf{A}}(\mathbf{r}(t))^2$ term, which leads to [19]

$$\hat{H} \approx \frac{\hat{\mathbf{p}}^2}{2m_0} + \sum_{\mathbf{k},j} \hbar\omega_{\mathbf{k}} \hat{a}^\dagger_{\mathbf{k},j}\hat{a}_{\mathbf{k},j} - \frac{q}{m_0}\hat{\mathbf{p}}\cdot\hat{\mathbf{A}}(\mathbf{r}(t)). \tag{4}$$

II. CALCULATION OF THE PARTIALLY TRACED STATE

Our main object of the study is a partially traced state, with a part of the field included in the description:

$$\varrho_{S:F_{\mathrm{obs}}}(t) \equiv tr_{F_{\mathrm{unob}}}[U_{S:F}(t)\varrho_0 U_{S:F}(t)^\dagger], \tag{5}$$

where S is the charge, and F_{obs} and F_{unob} denote the observed and unobserved modes, respectively, and $U_{S:F}(t)$ is the evolution operator corresponding to Eq. (4). The latter can be found exactly (cf. Eqs. (8) and (A12) in [12]; a similar derivation can be found also in [16]) and is given in the interaction picture by

$$\hat{U}^I_{S:F}(t) = \int d^3p |\mathbf{p}\rangle\langle\mathbf{p}| \otimes \hat{U}^I_F(t;\mathbf{p}), \tag{6}$$

which is a controlled-unitary type of evolution [14] (see also [20–22]) with

$$\hat{U}^I_F(t;\mathbf{p}) \equiv e^{i\sum_{\mathbf{k},j} C_{\mathbf{k}}\mathbf{p}\cdot\boldsymbol{\epsilon}_{\mathbf{k},j}\xi_{\mathbf{k}}(t)}\hat{D}\left(\sum_{\mathbf{k},j} C_{\mathbf{k}}\mathbf{p}\cdot\boldsymbol{\epsilon}_{\mathbf{k},j}\alpha_{\mathbf{k}}(t)\right). \tag{7}$$

where $\hat{D}(\sum_{\mathbf{k},j}\beta_{\mathbf{k},j}) \equiv \exp[\sum_{\mathbf{k},j}(\beta_{\mathbf{k},j}\hat{a}^\dagger_{\mathbf{k},j} - \beta^*_{\mathbf{k},j}\hat{a}_{\mathbf{k},j})]$ is the multimode displacement operator, $C_{\mathbf{k}} \equiv -(q/m_0)\sqrt{\hbar/(2\varepsilon_0\omega_{\mathbf{k}}V)}$ is a coupling coefficient,

$$\alpha_{\mathbf{k}}(t) \equiv e^{-i\mathbf{k}\cdot\mathbf{r}_0}\frac{1 - e^{i(\omega_{\mathbf{k}} - \mathbf{k}\cdot\mathbf{v}_0)t}}{\hbar(\omega_{\mathbf{k}} - \mathbf{k}\cdot\mathbf{v}_0)}, \tag{8}$$

and $\xi_{\mathbf{k}}(t) \equiv [t - \sin(\mathbf{k}\cdot\mathbf{v}_0 t)/(\mathbf{k}\cdot\mathbf{v}_0)]/(\omega_{\mathbf{k}} - \mathbf{k}\cdot\mathbf{v}_0)$ is a dynamical phase, which turns out to be irrelevant for our considerations. Note also that, since $\hat{\mathbf{p}}$ commutes with Eq. (4), the momentum of the charge is conserved during the evolution in the dipole approximation, so that in particular the momentum spread is constant in time.

Following the standard approach, the charge-field system is assumed to be initially in a product state [12,19]:

$$\varrho_0 = |\psi_{0S}\rangle\langle\psi_{0S}| \otimes \varrho_{0F}, \tag{9}$$

where $|\psi_{0S}\rangle$ is a charge initial wave packet and the field is in a thermal state, $\varrho_{0F} = \exp(-\beta\hat{H}_F)/Z(\beta)$, $\hat{H}_F \equiv \sum_{\mathbf{k},j}\hbar\omega_{\mathbf{k}}\hat{a}^\dagger_{\mathbf{k},j}\hat{a}_{\mathbf{k},j}$, and $\beta \equiv \hbar/k_B T$. This (to some extent artificially) decoupled state leads at the very short time scale $t \sim \bar{\Omega}^{-1}$ to the well-known effects of dressing and charge energy renormalization [12,19]. To separate those transient effects from the thermal influence, in what follows we assume the low thermal energy regime [12]:

$$k_B T \ll \hbar\bar{\Omega}. \tag{10}$$

The spreads of the initial wave packet $|\psi_{0S}\rangle$ are assumed to satisfy $\delta r_0 \ll c/\bar{\Omega}$ and obviously $\delta p_0 \ll m_0 c$, which warrants the moving dipole approximation for times [Eq. (3)] $\tau_{\mathrm{dip}} \gg \bar{\Omega}^{-1}$. However, as made clear later, δp_0 cannot be chosen too small either.

Under the above conditions, one can find the partially traced state (5) using Eqs. (B6) and (7). Although Eq. (B6) is formally written with the integral and the sharp momentum eigenstates, one should keep in mind that by the spectral theorem it is in fact a limit over finite divisions $\{\Delta\}$ of the momentum space $\mathbf{R}^3$, of sums with $|\mathbf{p}\rangle\langle\mathbf{p}|$ approximated by the spectral projectors $\hat{\Pi}_\Delta$. We thus obtain that in the interaction picture:

$$\varrho^I_{S:F_{\mathrm{obs}}}(t) = \sum_\Delta \hat{\Pi}_\Delta\varrho^I_{0S}\hat{\Pi}_\Delta \otimes \varrho^I_{F_{\mathrm{obs}}}(t;\mathbf{p}_\Delta) + \sum_{\Delta\neq\Delta'} D_{\mathbf{p}_\Delta,\mathbf{p}_{\Delta'}} \times \hat{\Pi}_\Delta\varrho^I_{0S}\hat{\Pi}_{\Delta'} \otimes \hat{U}^I_{F_{\mathrm{obs}}}(t;\mathbf{p}_\Delta)\varrho^I_{0F_{\mathrm{obs}}}\hat{U}^I_{F_{\mathrm{obs}}}(t;\mathbf{p}_{\Delta'})^\dagger, \tag{11}$$

where $\mathbf{p}_\Delta$ is some point from Δ, $\varrho_{0F_{\mathrm{obs}}} \equiv \mathrm{tr}_{\mathrm{unob}}\varrho_{0F}$, $\hat{U}_{F_{\mathrm{obs}}}(t;\mathbf{p}) \equiv \mathrm{tr}_{\mathrm{unob}}\hat{U}_F(t;\mathbf{p})$ [cf. Eq. (7)], and

$$\varrho^I_{F_{\mathrm{obs}}}(t;\mathbf{p}) \equiv \hat{U}^I_{F_{\mathrm{obs}}}(t;\mathbf{p})\varrho_{0F_{\mathrm{obs}}}\hat{U}^I_{F_{\mathrm{obs}}}(t;\mathbf{p})^\dagger, \tag{12}$$

$$D_{\mathbf{p},\mathbf{p}'}(t) \equiv \mathrm{tr}[\hat{U}_{F_{\mathrm{unob}}}(t;\mathbf{p})\varrho_{0F_{\mathrm{unob}}}\hat{U}_{F_{\mathrm{unob}}}(t;\mathbf{p}')^\dagger] \tag{13}$$

$$\equiv \exp[-\Gamma_{\mathbf{p},\mathbf{p}'}(t) + i\Phi_{\mathbf{p},\mathbf{p}'}(t)], \tag{14}$$

the latter being the decoherence factor due to the unobserved field modes (the same in the interaction and the Schrödinger pictures). The real part $\Gamma_{\mathbf{p},\mathbf{p}'}(t)$ leads to the damping of coherences in the momentum basis and singles it out as the pointer basis. The resulting suppression of the charge-field entanglement is a necessary condition for the appearance of objectivity [14,15].

III. DECOHERENCE PROCESSES

The decoherence process in this model was extensively studied in [12] with the whole of the radiation traced out. The results can be easily generalized to our situation where only a portion F_{unob} of the modes is neglected. We assume it is macroscopic, i.e., contains a large enough number of modes to pass to the continuum limit $\sum_{\mathbf{k}} \to V\int_{F_{\mathrm{unob}}} d^3k/(2\pi)^3$, where F_{unob} is described by an angle Ω_{unob} of the unobserved directions (see Fig. 1), containing all the relevant frequencies

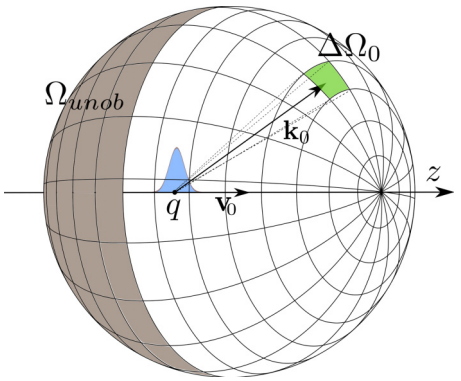

FIG. 1. The considered physical model. A nonrelativistic charged particle interacts with an electromagnetic field, treated as the environment. The particle is described by a wave packet, narrow compared to the shortest relevant radiation wavelength, and moves with initial velocity $\mathbf{v}_0$, chosen along the z axis. The sphere represents the "celestial sphere" of the mode directions $\mathbf{k}/k$. A part of this sphere, given by a solid angle Ω_{unob}, is not monitored and the corresponding modes are traced out. The rest is divided into small portions (only one portion shown) $\Delta\Omega_0$, centered each around some average direction $\mathbf{k}_0/k_0$, which represent, e.g., detection regions of approximately pointlike detectors.

and polarizations. Using $k_BT \ll \hbar\bar{\Omega}$ and $v_0/c \ll 1$ we obtain

$$\frac{\pi}{\alpha}\Gamma_{\mathbf{p},\mathbf{p}'}(t) = \left[F_0(\Delta\mathbf{p}) + \frac{v_0}{c}F_1(\Delta\mathbf{p})\right] \times \ln\left[\sqrt{1+\bar{\Omega}^2t^2}\,\frac{\sinh(t/\tau_F)}{t/\tau_F}\right] - \frac{v_0}{2c}F_1(\Delta\mathbf{p})\left[\frac{t}{\tau_F}\coth\frac{t}{\tau_F} - \frac{1}{1+\bar{\Omega}^2t^2}\right] + O\left(\frac{v_0^2}{c^2}\right), \tag{15}$$

where $\alpha \equiv q^2/(4\pi\varepsilon_0\hbar c)$ is proportional to the fine structure constant, $\tau_F \equiv \hbar/(\pi k_BT)$ is the characteristic thermal time, $\Delta\mathbf{p} \equiv \mathbf{p} - \mathbf{p}'$, and

$$F_0(\Delta\mathbf{p}) \equiv \frac{1}{(m_0c)^2}\int_{\Omega_{\text{unob}}}\frac{d\Omega_{\mathbf{k}}}{4\pi}\Delta\mathbf{p}^2_{\perp\mathbf{k}}, \tag{16}$$

$$F_1(\Delta\mathbf{p}) \equiv \frac{2}{(m_0c)^2}\int_{\Omega_{\text{unob}}}\frac{d\Omega_{\mathbf{k}}}{4\pi}\cos\theta_{\mathbf{k}}\Delta\mathbf{p}^2_{\perp\mathbf{k}}. \tag{17}$$

Here $F_0(\Delta\mathbf{p})$ and $F_1(\Delta\mathbf{p})$ are the average and the "first moment" of the squared norm of the transversal part of $\Delta\mathbf{p}$, $\Delta\mathbf{p}^2_{\perp\mathbf{k}} \equiv \sum_{ij}\Delta\mathbf{p}_i\Delta\mathbf{p}_j(\delta_{ij} - k_ik_j/k^2)$, over the unobserved directions Ω_{unob} and rescaled to $(m_0c)^2$. A comment is in order. The quantities (16) and (17) are formally second order in $1/c$. This is, however, not a mismatch in the relativistic expansion as it may first appear due to the nonrelativistic Hamiltonian used. This is rather a result of the continuum limit and the wave nature of light as we illustrate in more detail in Appendix B.

Since generically $F_1(\Delta\mathbf{p}) \neq 0$, there is in general a nonvanishing first-order contribution to the decoherence factor from the Doppler shift [cf. Eq. (8)]. If, however, all of the field is neglected, $F_1(\Delta\mathbf{p}) = 0$ [12] and in the first order Eq. (15) is the same as for a static wave packet ($\mathbf{v}_0 = 0$). One easily sees from Eq. (15) that the decoherence factor depends on the time via $\bar{\Omega}t$ and t/τ_F. This defines three time-dependence regimes, with the following approximate behavior in each of them [12]:

$$\frac{\pi}{\alpha}\Gamma_{\mathbf{p},\mathbf{p}'}(t) \approx \begin{cases} F_0\frac{\bar{\Omega}^2t^2}{2}, & t \ll \bar{\Omega}^{-1} \\ \left(F_0 + \frac{v_0}{c}F_1\right)\ln\bar{\Omega}t - \frac{v_0}{2c}F_1, & \bar{\Omega}^{-1} \ll t \ll \tau_F \\ \left(F_0 + \frac{v_0}{2c}F_1\right)\frac{t}{\tau_F} + \left(F_0 + \frac{v_0}{c}F_1\right)\ln\bar{\Omega}\tau_F, & t \gg \tau_F. \end{cases} \tag{18}$$

The initial "vacuum decoherence" for $t \ll \tau_F$, accompanying the dressing and the mass renormalization [12], is a consequence of the artificially decoupled initial state (9). Past this transient period, for $t \sim \tau_F$ the thermally driven decoherence begins, giving the exponential decay of coherences with time. Since $\tau_{\text{dip}}/\tau_F = (m_0c/\delta p_0)(k_BT/\hbar\Omega)$, one can achieve $\tau_F < \tau_{\text{dip}}$ in the studied regime so that it can be in principle observed within the dipole approximation. However, while the fundamental time limit (3), imposed by the wave packet spread, grows linearly with $m_0c/\delta p_0$, the decoherence factor decays only as $|D_{\mathbf{p},\mathbf{p}'}| \sim \exp[-\alpha(m_0c/\delta p_0)^{-2}]$, since from Eqs. (16) and (17), $F_0(\Delta\mathbf{p}), F_1(\Delta\mathbf{p}) \sim (m_0c/\delta p_0)^{-2}$. Thus, what is required is a not-so-small momentum spread and a very strong coupling, $\alpha \gg 1$, corresponding to macroscopic charges. A sample plot of such a situation is shown in Fig. 2.

IV. INFORMATION CONTENT OF THE RADIATION FIELD

We now move to the most interesting part—the information content of the observed radiation modes [Eq. (12)], which has not been studied explicitly in this model. Let us first look at an individual mode $\boldsymbol{\epsilon}_{\mathbf{k},j}$. From Eqs. (7) and (11) its state is a mixture of displaced initial thermal states:

$$\varrho^I_{\mathbf{k},j}(t;\mathbf{p}) \equiv \hat{D}_{\mathbf{p}\cdot\boldsymbol{\epsilon}_{\mathbf{k},j}}(t)\varrho_{0\mathbf{k},j}\hat{D}_{\mathbf{p}\cdot\boldsymbol{\epsilon}_{\mathbf{k},j}}(t)^\dagger, \tag{19}$$

where $\hat{D}_{\mathbf{p}\cdot\boldsymbol{\epsilon}_{\mathbf{k},j}}(t)$ stands for each of the displacements in Eq. (7). These displacements depend on the component of the charge momentum along the mode polarization and we can ask how distinguishable are two such states for different $\mathbf{p}\cdot\boldsymbol{\epsilon}_{\mathbf{k},j}$. As the appropriate measure, we choose the mixed-state fidelity (also known as generalized overlap) $B(\varrho,\sigma) \equiv \text{tr}\sqrt{\sqrt{\varrho}\sigma\sqrt{\varrho}}$ [14,23], satisfying $B(\varrho,\sigma) = 0$ if and only if ϱ and σ have

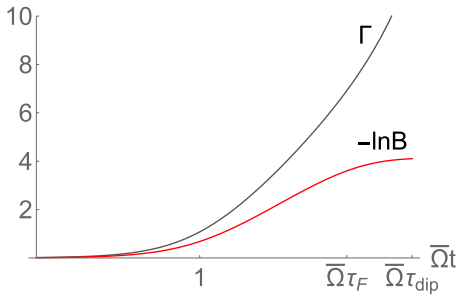

FIG. 2. A sample plot of the decoherence damping factor $\Gamma_{\mathbf{p},\mathbf{p}'}(t)$ (upper trace) and the state fidelity $-\ln B^{\mathrm{mac}}_{\mathbf{p},\mathbf{p}'}(t)$ (lower trace) as a function of time, measured in the inverse cutoff units $\bar{\Omega}^{-1}$ and plotted on a logarithmic scale. The parameters for the plot are the following: $\bar{\Omega} = 10^{15}$ s^{-1}, $\alpha = 10^5$, $\delta p_0/(m_0 c) = 5 \times 10^{-2}$, $\hbar\bar{\Omega}/(k_B T) = 4 \times 10^2$, the unobserved portion Ω_{unob} is given by $0 \leqslant \theta \leqslant \pi/4$, and the observed macrofraction size is $\Delta\Omega_0/(4\pi) = 0.05$. This gives $\tau_{\mathrm{dip}} = 20\ \bar{\Omega}^{-1}$ and $\tau_F \approx 7.95\ \bar{\Omega}^{-1}$.

orthogonal supports and hence are perfectly distinguishable. $B[\varrho_{\mathbf{k},j}(t;\mathbf{p}),\varrho_{\mathbf{k},j}(t;\mathbf{p}')] \equiv B^{(\mathbf{k},j)}_{\mathbf{p},\mathbf{p}'}(t)$ can be calculated using, e.g., the techniques of [16] and reads [24]

$$\ln B^{(\mathbf{k},j)}_{\mathbf{p},\mathbf{p}'}(t) = -\frac{\alpha\pi\hbar^2 c(\boldsymbol{\epsilon}_{\mathbf{k},j}\cdot\Delta\mathbf{p})^2}{m_0^2\omega_{\mathbf{k}}V}|\alpha_{\mathbf{k}}(t)|^2\tanh\left(\frac{\beta\omega_k}{2}\right). \tag{20}$$

If $\boldsymbol{\epsilon}_{\mathbf{k},j}\cdot\Delta\mathbf{p} \neq 0$, Eq. (8) implies that it oscillates with a Doppler-shifted frequency $\omega_{\mathbf{k}}[1-\mathbf{k}\cdot\mathbf{v}_0/(kc)]$. However, in the infrared limit $V\to\infty$, $B^{(\mathbf{k},j)}_{\mathbf{p},\mathbf{p}'}(t)\to 1$, indicating that the states (19) become identical for all $\mathbf{p}$. Thus, at the microscopic level each field mode carries vanishingly small information about the charge (cf. [14]).

Let us now introduce and study so-called macrofractions of the field [14,25–28]. We divide the monitored directions Ω_{obs} into patches Ω_{mac}, each containing a large enough number of modes to justify the continuum limit. The collection of all modes within Ω_{mac} with a fixed polarization defines a macrofraction with a given polarization. Such a coarse graining of the observed portion of the field may correspond, e.g., to an array of (polarization-sensitive, wideband) detectors; see Fig. 1. In the box quantization, a state of a macrofraction can be formally written as

$$\varrho^{(j)}_{\mathrm{mac}}(t;\mathbf{p}) \equiv \bigotimes_{\mathbf{k}/k\in\Omega_{\mathrm{mac}}}\ \bigotimes_{\omega_{\mathbf{k}}\lesssim\Omega} \varrho_{\mathbf{k},j}(t;\mathbf{p}). \tag{21}$$

We are interested in the mixed-state fidelity $B[\varrho^{(j)}_{\mathrm{mac}}(t;\mathbf{p}),\varrho^{(j)}_{\mathrm{mac}}(t;\mathbf{p}')] \equiv B^{\mathrm{mac}}_{\mathbf{p},\mathbf{p}',j}(t)$ for a fixed polarization j. Since $B(\varrho^{\otimes n},\sigma^{\otimes n})$ factorizes with respect to the tensor product, $B^{\mathrm{mac}}_{\mathbf{p},\mathbf{p}',j}(t)$ is a product taken over the macrofraction of the terms (20). Passing to the continuum limit and imposing the cutoff, we obtain

$$\begin{aligned}\ln B^{\mathrm{mac}}_{\mathbf{p},\mathbf{p}',j}(t) &= -\frac{\alpha}{\pi(m_0c)^2}\int\frac{d\omega}{\omega}e^{-\frac{\omega}{\bar{\Omega}}}\tanh\left(\frac{\beta\omega}{2}\right)\\ &\int_{\Omega_{\mathrm{mac}}}\frac{d\Omega_{\mathbf{k}}}{4\pi}(\boldsymbol{\epsilon}_{\mathbf{k},j}\cdot\Delta\mathbf{p})^2\frac{1-\cos[(\omega-\mathbf{k}\cdot\mathbf{v}_0)t]}{[1-\mathbf{k}\cdot\mathbf{v}_0/(kc)]^2}.\end{aligned} \tag{22}$$

We are particularly interested in the information content of small macrofractions, described by a small angle $\Delta\Omega_0$ centered around some $\mathbf{k}_0$ (see Fig. 1). It corresponds to an almost pointlike (from the macroscopic point of view) detector [29]. We may then approximate $\int_{\Delta\Omega_0} d\Omega_{\mathbf{k}} f(\mathbf{k}) \approx f(\mathbf{k}_0)\Delta\Omega_0$ and the remaining frequency integral can be calculated for $k_B T \ll \hbar\bar{\Omega}$, yielding

$$\begin{aligned}\ln B^{\mathrm{mac}}_{\mathbf{p},\mathbf{p}',j}(t) = &-\frac{\alpha\Delta\Omega_0(\boldsymbol{\epsilon}_{\mathbf{k}_0,j}\cdot\Delta\mathbf{p})^2}{4\pi^2(m_0c)^2}\\ &\frac{1}{\nu^2}\ln\left[\sqrt{1+\nu^2\bar{\Omega}^2t^2}\,\frac{\tanh(\nu t/\tau_F)}{\nu t/\tau_F}\right],\end{aligned} \tag{23}$$

where

$$\nu \equiv [1-\mathbf{k}_0\cdot\mathbf{v}_0/(k_0c)] \tag{24}$$

is the Doppler factor along the direction of $\mathbf{k}_0$. Let us compare the behavior of Eq. (23) with that of the decoherence factor. Performing the same approximations as in Eq. (18) yields

$$\begin{aligned}&-\left[\frac{\alpha\Delta\Omega_0(\boldsymbol{\epsilon}_{\mathbf{k}_0,j}\cdot\Delta\mathbf{p})^2}{4\pi^2(m_0c)^2}\right]^{-1}\ln B^{\mathrm{mac}}_{\mathbf{p},\mathbf{p}'}(t)\\ &\approx\begin{cases}\frac{\bar{\Omega}^2t^2}{2}, & t\ll\bar{\Omega}^{-1}\\ \frac{1}{\nu^2}\ln(\nu\bar{\Omega}t), & \bar{\Omega}^{-1}\ll t\ll\tau_F\\ \frac{1}{\nu^2}\ln(\bar{\Omega}\tau_F), & t\gg\tau_F.\end{cases}\end{aligned} \tag{25}$$

We see that modulo the geometric factor (controlled by the solid angle of the directions), the behavior of distinguishability, as measured by the above state fidelity, and decoherence is the same up to $t\sim\tau_F$; i.e., during the dressing the field acquires information about the momentum at a similar rate as it decoheres the charge. Past this time, the decoherence factor keeps decreasing [Eq. (18)], but the state distinguishability stabilizes at

$$B^{\mathrm{mac}}_{\infty} \sim [\bar{\Omega}\tau_F]^{-\alpha(\frac{\Delta p}{m_0c})^2}. \tag{26}$$

The reason is that the cutoff limits the energy available for the displacement (7) of the initial thermal state during the evolution. Since this displacement encodes the momentum data into the field, the cutoff puts a fundamental limit on the accuracy with which the information about the momentum can be imprinted in and extracted from the thermal field [30]. It is worth stressing that in our setup this is a thermal effect—for the field initially in the vacuum state, B^{mac} decays without a limit, as follows from Eq. (23) with $T=0$. The accuracy is determined by Eq. (26) and depends, among other things, on the ratio of the cutoff and the thermal energies as $\bar{\Omega}\tau_F = \hbar\bar{\Omega}/(k_B T)$. The latter is small in the low-energy regime considered here; however, looking at the exponent in Eq. (26) a similar remark as after Eq. (18) applies: the momentum difference to be discriminated cannot be arbitrarily small and a very strong coupling, $\alpha\gg 1$, is required for state fidelity to be small. This can be achieved, along with a vanishing decoherence factor, as shown in Fig. 2.

For convenience, let us summarize the different time behaviors from Eqs. (18) and (25) in the following table, where $f(\Delta\mathbf{p}) \equiv \frac{\alpha\Delta\Omega_0(\boldsymbol{\epsilon}_{\mathbf{k}_0,j}\cdot\Delta\mathbf{p})^2}{4\pi^2(m_0c)^2}$, ν is the Doppler factor given by Eq. (24), and $F_0(\Delta\mathbf{p})$, $F_1(\Delta\mathbf{p})$ by Eqs. (16) and (17):

Time scale	Log of the modulus of decoherence factor	Log of the state fidelity
$t \ll \bar{\Omega}^{-1}$ (time-dependent dressing)	$F_0(\Delta\mathbf{p})\frac{\bar{\Omega}^2 t^2}{2}$	$f(\Delta\mathbf{p})\frac{\bar{\Omega}^2 t^2}{2}$
$\bar{\Omega}^{-1} \ll t \ll \tau_F$ (vacuum decoherence)	$\ln(\bar{\Omega}t)[F_0(\Delta\mathbf{p}) + \frac{v_0}{c}F_1(\Delta\mathbf{p})] - \frac{v_0}{2c}F_1(\Delta\mathbf{p})$	$\frac{f(\Delta\mathbf{p})}{\nu^2}\ln(\nu\bar{\Omega}t)$
$t \gg \tau_F$ (thermal decoherence)	$\frac{t}{\tau_F}[F_0(\Delta\mathbf{p}) + \frac{v_0}{2c}F_1(\Delta\mathbf{p})] + [F_0(\Delta\mathbf{p}) + \frac{v_0}{c}F_1(\Delta\mathbf{p})]\ln(\bar{\Omega}\tau_F)$	$\frac{f(\Delta\mathbf{p})}{\nu^2}\ln(\bar{\Omega}\tau_F)$

It implies that in the discussed parameter regime, the partially traced state (5) approaches the so-called spectrum broadcast structure [14,15] and by the results of [15] provides a form of objectivization of the charge momentum. Let us elaborate on that. SBS is defined as the following maximally correlated, classical-classical [31,32] state (cf. [20,33,34]):

$$\varrho = \sum_i p_i |i\rangle\langle i| \otimes \varrho_i^{(1)} \otimes \cdots \otimes \varrho_i^{(M)}, \tag{27}$$

where $|i\rangle$ is some basis (called a pointer basis) in the system space, p_i are probabilities and states $\varrho_i^{(m)}$, $m = 1,\ldots,M$, have vanishing state fidelity for different i's, and $B[\varrho_i^{(m)},\varrho_{i'\neq i}^{(m)}] = 0$ for all m. It has an important property wherein measuring the supports of $\varrho_i^{(m)}$ all the observers $m = 1,\ldots,M$ obtain the same index i with the same probabilities p_i in perfect correlation with the state of the system $|i\rangle$ and without disturbing (after forgetting the results) the whole state $\varrho_{S:F_{\rm obs}}$. In this sense the information about the state of the system is redundantly encoded in the environment and can be extracted without perturbation. This, in turn, is at the core of what we perceive as objectivity [4,15]. Returning to the studied situation, vanishing of the decoherence factor and the state fidelities implies [14] that past τ_F the state (5) is approximately of the form (somewhat abusing the notation and using the continuous distribution for $\mathbf{p}$)

$$\varrho_{S:F_{\rm obs}}(t) \approx \int d^3p |\langle\mathbf{p}|\psi_{0S}\rangle|^2 |\mathbf{p}\rangle\langle\mathbf{p}| \bigotimes_j \left[\varrho^{(j)}_{{\rm mac}_{\mathbf{k}_0}}(t;\mathbf{p}) \otimes \varrho^{(j)}_{{\rm mac}_{\mathbf{k}_1}}(t;\mathbf{p}) \otimes \cdots\right], \tag{28}$$

where directions $\mathbf{k}_0,\mathbf{k}_1,\ldots$ define the macrofractions into which the observed radiation is divided and their states $\varrho^{(j)}_{{\rm mac}_{\mathbf{k}}}(t;\mathbf{p})$ have small state fidelities (26) for different momenta. Thus, although various types of quantum correlations, including entanglement, are produced during the evolution, the ones that survive after a sufficiently long time, the partial loss of the field, and the coarse graining are only of the SBS type. However, although formally resembling an SBS, there is a key difference between Eqs. (28) and (27) and the structures encountered so far [14,16,17] [apart from the limit on the accuracy, Eq. (26)]. By Eqs. (7), (19), and (21) what is in fact encoded in each $\varrho^{(j)}_{{\rm mac}_{\mathbf{k}}}(t;\mathbf{p})$ is the momentum component $\boldsymbol{\epsilon}_{\mathbf{k},j}\cdot\mathbf{p}$ along the average macrofraction polarization vector corresponding to polarization j. Thus, each macrofraction carries in general different information about the same quantity $\mathbf{p}$. This situation resembles seeing different pieces of the same object. However, picking two different macrofractions, centered around $\mathbf{k}_0,\mathbf{k}_1$ which are not antipodal, it is possible to choose three linearly independent polarizations $\boldsymbol{\epsilon}_1,\boldsymbol{\epsilon}_2,\boldsymbol{\epsilon}_3$. Then, $\mathbf{p}$ can be reconstructed from $\boldsymbol{\epsilon}_i\cdot\mathbf{p}$ using the Gramm matrix $G_{rs} \equiv \boldsymbol{\epsilon}_r\cdot\boldsymbol{\epsilon}_s$: $\mathbf{p} = \sum G^{-1}_{rs}(\boldsymbol{\epsilon}_s\cdot\mathbf{p})\boldsymbol{\epsilon}_s$. In other words, any triple of polarization macrofractions in Eq. (28) with linearly independent polarization vectors encodes almost perfect information about the charge momentum $\mathbf{p}$. If we now imagine that the observed "celestial sphere" $\Omega_{\rm obs}$ can be divided into a very large number of infinitesimal macrofractions $\Delta\Omega$, then it is clear that the information about $\mathbf{p}$ is encoded with a huge redundancy in the field. Moreover, it is available to multiple observers without disturbing the state of the system (modulo the finite accuracy discussed above [35]). In this sense, the field in the studied regime provides an objectivization of the charge momentum.

V. CONCLUDING REMARKS

Our studies may be viewed as a step towards a more fundamental rederivation, on the level of QED, of the results on objectivity [14,27] in the celebrated phenomenological model of decoherence due to environmental scattering [36]. However, due to the used dipole approximation what becomes objective here is the momentum rather than the position. In the context of a free charge, this approximation is the biggest limitation and a natural direction would be to go beyond it. Another perspective would be systems with internal degrees of freedom, e.g., qubit models within QED [37].

Finally, since we are explicitly including a part of the environment in the description, it may seem that we are dealing with a non-Markovian evolution, where the role of the environment cannot be simplified to the usual Markovian generator. This is is not necessarily so; the reason for including the environment in the present description is to study the information content of the environment and not because its presence cannot be described in simple terms. The relation between spectrum broadcast structures and properly defined non-Markovianity was studied in [38] (cf. [39]). There seems to be no obvious connection between the two, at least in the context of the spin-boson model.

ACKNOWLEDGMENTS

We would like to thank R. and P. Horodecki, D. Chruściński, K. Rzażewski, I. Białynicki-Birula, and especially J. Karwowski for discussions. We acknowledge the financial support of the John Templeton Foundation through Grant No. 56033.

APPENDIX A: DERIVATION OF THE DECOHERENCE FACTOR

Here we present the derivation leading to Eq. (15) in the main text. It is a generalization of the derivation presented in [12] taking into account that in the present case only a portion F_{unob} of the field modes is unobserved. From Eqs. (14) and (7), we have

$$\begin{aligned}-\Gamma_{\mathbf{p},\mathbf{p}'}(t) &= \ln|D_{\mathbf{p},\mathbf{p}'}(t)| \\ &= \ln|\mathrm{tr}[\hat{U}_{F_{\text{unob}}}(t;\mathbf{p})\varrho_{0F_{\text{unob}}}\hat{U}_{F_{\text{unob}}}(t;\mathbf{p}')^{\dagger}]| \\ &= \ln\left|\mathrm{tr}\left[\hat{D}\left(\sum_{\mathbf{k}_{\text{unob}},j} C_{\mathbf{k}}\Delta\mathbf{p}\cdot\boldsymbol{\epsilon}_{\mathbf{k},j}\alpha_{\mathbf{k}}(t)\right)\varrho_{0F_{\text{unob}}}\right]\right|. \end{aligned} \tag{A1}$$

If the environment is initially in a thermal state $\varrho_{0F} = \exp(-\beta\hat{H}_F)/Z(\beta)$ one finds [9,12,16]

$$\begin{aligned}&-\Gamma_{\mathbf{p},\mathbf{p}'}(t) \\ &= \frac{1}{2}\sum_{\mathbf{k}_{\text{unob}},j}|C_{\mathbf{k}}\alpha_{\mathbf{k}}(t)x|^2\left|\Delta\mathbf{p}\cdot\boldsymbol{\epsilon}_{\mathbf{k},j}\right|^2\coth\left(\frac{\beta\omega_k}{2}\right),\end{aligned} \tag{A2}$$

with

$$|C_{\mathbf{k}}\alpha_{\mathbf{k}}(t)|^2 = \frac{2\pi q^2}{\hbar\omega_{\mathbf{k}}^3 m_0^2 V}\frac{1-\cos\{\omega_{\mathbf{k}}t[1-\mathbf{k}\cdot\mathbf{v}_0/(kc)]\}}{[1-\mathbf{k}\cdot\mathbf{v}_0/(kc)]^2}.$$

Subsequently, we assume that the number of field modes in the unobserved fraction is large enough to pass to the continuum limit; i.e., the sum over modes is replaced by an integral

$$\begin{aligned}\sum_{\mathbf{k}} \to V\int_{F_{\text{unob}}}\frac{d^3k}{(2\pi)^3} &= \frac{V}{2\pi^2}\int_0^{\infty}k^2dk\int_{\Omega_{\text{unob}}}\frac{d\Omega_{\mathbf{k}}}{4\pi} \\ &= \frac{V}{2\pi^2c^3}\int_0^{\infty}\omega^2d\omega\int_{\Omega_{\text{unob}}}\frac{d\Omega_{\mathbf{k}}}{4\pi}.\end{aligned} \tag{A3}$$

In the above expression, the unobserved field modes $\mathbf{k}\in F_{\text{unob}}$ are expressed in terms of spherical coordinates: the wave vector length $k=\omega/c$ and an angle Ω_{unob} of the unobserved directions (see Fig. 1 in the main text). Please note that the appearance of the speed of light c here is a result of the dispersion relation $\omega = kc$. Equation (A2) takes the form

$$-\Gamma_{\mathbf{p},\mathbf{p}'}(t) = \frac{\alpha/\pi}{(m_0c)^2}\int_0^{\infty}\frac{d\omega}{\omega}\int_{\Omega_{\text{unob}}}\frac{d\Omega_{\mathbf{k}}}{4\pi}e^{-\frac{\omega}{\Omega}}\coth\left(\frac{\beta\omega}{2}\right), \tag{A4}$$

$$\frac{1-\cos\{\omega t[1-\mathbf{k}\cdot\mathbf{v}_0/(kc)]\}}{[1-\mathbf{k}\cdot\mathbf{v}_0/(kc)]^2}\sum_j|\Delta\mathbf{p}\cdot\boldsymbol{\epsilon}_{\mathbf{k},j}|^2, \tag{A5}$$

where additionally the cutoff was introduced. The next step is to expand the fraction under the integral in a series with respect to $\frac{\mathbf{k}/k\cdot\mathbf{v}_0}{c}\equiv\frac{v_0}{c}\cos\theta_{\boldsymbol{k}}$:

$$\begin{aligned}&\frac{1-\cos\{\omega t[1-(v_0/c)\cos\theta_{\boldsymbol{k}}]\}}{[1-(v_0/c)\cos\theta_{\boldsymbol{k}}]^2} \\ &\approx(1-\cos(\omega t))\left(1+2\frac{v_0}{c}\cos\theta_{\boldsymbol{k}}+3\left(\frac{v_0}{c}\cos\theta_{\boldsymbol{k}}\right)^2\right) \\ &\quad-\omega t\sin(\omega t)\frac{v_0}{c}\cos\theta_{\boldsymbol{k}}\left(1+2\frac{v_0}{c}\cos\theta_{\boldsymbol{k}}\right) \\ &\quad+(\omega t)^2\cos(\omega t)\left(\frac{v_0}{c}\cos\theta_{\boldsymbol{k}}\right)^2+O\left(\frac{v_0^3}{c^3}\right).\end{aligned} \tag{A6}$$

Using the identity for polarization vectors

$$\sum_j\boldsymbol{\epsilon}_{\boldsymbol{k},j}^n\boldsymbol{\epsilon}_{\boldsymbol{k},j}^m = \delta_{mn}-\mathbf{k}_n\mathbf{k}_m/k^2, \tag{A7}$$

one easily establishes that

$$|\Delta\mathbf{p}\cdot\boldsymbol{\epsilon}_{\mathbf{k},j}|^2 = \sum_{ij}\Delta\mathbf{p}_i\Delta\mathbf{p}_j(\delta_{ij}-k_ik_j/k^2)\equiv\Delta\mathbf{p}_{\perp\mathbf{k}}^2. \tag{A8}$$

Inserting Eqs. (A6) and (A8) into Eq. (A4) leads to

$$\begin{aligned}\frac{\pi}{\alpha}\Gamma_{\mathbf{p},\mathbf{p}'}(t) &= \left[F_0(\Delta\mathbf{p})+\frac{v_0}{c}F_1(\Delta\mathbf{p})\right] \\ &\quad\times\int_0^{\infty}\frac{d\omega}{\omega}e^{-\frac{\omega}{\Omega}}\coth\left(\frac{\beta\omega}{2}\right)(1-\cos(\omega t)) \\ &\quad-\frac{v_0}{2c}F_1(\Delta\mathbf{p})t\int_0^{\infty}d\omega e^{-\frac{\omega}{\Omega}}\coth\left(\frac{\beta\omega}{2}\right)\sin(\omega t) \\ &\quad+O\left(\frac{v_0^2}{c^2}\right),\end{aligned} \tag{A9}$$

where

$$F_0(\Delta\mathbf{p}) \equiv \frac{1}{(m_0c)^2}\int_{\Omega_{\text{unob}}}\frac{d\Omega_{\mathbf{k}}}{4\pi}\Delta\mathbf{p}_{\perp\mathbf{k}}^2, \tag{A10}$$

$$F_1(\Delta\mathbf{p}) \equiv \frac{2}{(m_0c)^2}\int_{\Omega_{\text{unob}}}\frac{d\Omega_{\mathbf{k}}}{4\pi}\cos\theta_{\mathbf{k}}\Delta\mathbf{p}_{\perp\mathbf{k}}^2. \tag{A11}$$

The frequency integrals are split into vacuum and thermal contributions:

$$\begin{aligned}&\int_0^{\infty}\frac{d\omega}{\omega}e^{-\frac{\omega}{\Omega}}\coth\left(\frac{\beta\omega}{2}\right)(1-\cos(\omega t)) = \Gamma_1^{\text{vac}}+\Gamma_1^{\text{th}}, \\ &\Gamma_1^{\text{vac}} \equiv \int_0^{\infty}\frac{d\omega}{\omega}e^{-\frac{\omega}{\Omega}}(1-\cos(\omega t)), \\ &\Gamma_1^{\text{th}} \equiv \int_0^{\infty}\frac{d\omega}{\omega}e^{-\frac{\omega}{\Omega}}\left[\coth\left(\frac{\beta\omega}{2}\right)-1\right](1-\cos(\omega t)),\end{aligned} \tag{A12}$$

$$\begin{aligned}&\int_0^{\infty}d\omega e^{-\frac{\omega}{\Omega}}\coth\left(\frac{\beta\omega}{2}\right)\sin(\omega t) = \Gamma_2^{\text{vac}}+\Gamma_2^{\text{th}}, \\ &\Gamma_2^{\text{vac}} \equiv \int_0^{\infty}d\omega e^{-\frac{\omega}{\Omega}}\sin(\omega t), \\ &\Gamma_2^{\text{th}} \equiv \int_0^{\infty}d\omega e^{-\frac{\omega}{\Omega}}\left[\coth\left(\frac{\beta\omega}{2}\right)-1\right]\sin(\omega t).\end{aligned} \tag{A13}$$

Evaluation of vacuum contributions is straightforward:

$$\Gamma_1^{\text{vac}} = \tfrac{1}{2}\ln[1+(\bar{\Omega}t)^2], \tag{A14}$$

$$\Gamma_2^{\text{vac}} = \frac{(\bar{\Omega}t)^2}{1+(\bar{\Omega}t)^2}. \tag{A15}$$

To arrive at close formulas for thermal contribution, in both cases we need to assume that the energy scale set by cutoff is much larger than the thermal energy, i.e., $k_BT \ll \hbar\Omega$. Under

this assumption one finds

$$\Gamma_1^{\rm th} = \ln\left[\frac{\sinh(t/\tau_F)}{t/\tau_F}\right] \tag{A16}$$

$$\Gamma_2^{\rm th} = -\frac{1}{1+\bar{\Omega}^2 t^2}. \tag{A17}$$

Combining the above expressions with Eq. (A9) allows one to arrive at Eq. (15) of the main text.

Let us now briefly discuss the fidelity calculation. To arrive at Eq. (20), we used the derivation presented in [16]. Subsequently we approximate the angular integral $\int_{\Delta\Omega_0} d\Omega_{\mathbf{k}} f(\mathbf{k}) \approx f(\mathbf{k}_0)\Delta\Omega_0$ and split the frequency integral as

$$\frac{1}{\nu^2}\int \frac{d\omega}{\omega} e^{-\frac{\omega}{\Omega}} \tanh\left(\frac{\beta\omega}{2}\right)(1-\cos(\nu t)) = \frac{1}{\nu^2}(B^{\rm vac}+B^{\rm th}), \tag{A18}$$

where $\nu \equiv [1-\mathbf{k}_0\cdot\mathbf{v}_0/(k_0 c)]$. The vacuum part is the same as for the decoherence factor [Eqs. (A14) and (A15)],

$$B^{\rm vac} = \Gamma_1^{\rm vac}, \tag{A19}$$

whereas the thermal integral reads

$$B^{\rm th} = \ln\left[\frac{\tanh(\nu t/\tau_F)}{\nu t/\tau_F}\right]. \tag{A20}$$

APPENDIX B: INCLUSION OF HIGHER-ORDER RELATIVISTIC TERMS

Here we show that decoherence and fidelity are always two orders of magnitude higher than the Hamiltonian in a formal $1/c$ expansion. This, however, is not a result of the relativistic effects *per se*, but rather of the continuum limit and the dispersion relation for light. We show it by taking into account the first relativistic correction to the Hamiltonian (4). We start with the relativistic Hamiltonian

$$\hat{H} = m_0 c^2\sqrt{1+\frac{\hat{\boldsymbol{\pi}}^2}{m_0^2 c^2}} - m_0 c^2 + \sum_{\mathbf{k},j}\hbar\omega_{\mathbf{k}}\hat{a}^\dagger_{\mathbf{k},j}\hat{a}_{\mathbf{k},j}, \tag{B1}$$

with canonical momentum

$$\hat{\boldsymbol{\pi}} = \hat{\mathbf{p}} - \frac{q}{c}\hat{\mathbf{A}}(\hat{\mathbf{r}}). \tag{B2}$$

Expanding the square root up to $1/c^2$ we get

$$\hat{H} = \frac{\hat{\mathbf{p}}^2}{2m_0} - \frac{\hat{\mathbf{p}}^4}{8m_0^3 c^2} + \sum_{\mathbf{k},j}\hbar\omega_{\mathbf{k}}\hat{a}^\dagger_{\mathbf{k},j}\hat{a}_{\mathbf{k},j} - \frac{q}{m_0 c}\hat{\mathbf{p}}\cdot\hat{\mathbf{A}}(\hat{\mathbf{r}}) + \frac{q}{4m_0^3 c^3}(\hat{\mathbf{p}}^2\hat{\mathbf{p}}\cdot\hat{\mathbf{A}}(\hat{\mathbf{r}}) + \hat{\mathbf{p}}\cdot\hat{\mathbf{A}}(\hat{\mathbf{r}})\hat{\mathbf{p}}^2) + O(\hat{\mathbf{A}}^2(\hat{\mathbf{r}})). \tag{B3}$$

Subsequently we neglect terms proportional to $\hat{\mathbf{A}}(\hat{\mathbf{r}}(t))^2$ and use moving dipole approximation so that

$$\hat{H} \approx \frac{\hat{\mathbf{p}}^2}{2m_0} - \frac{\hat{\mathbf{p}}^4}{8m_0^3 c^2} + \sum_{\mathbf{k},j}\hbar\omega_{\mathbf{k}}\hat{a}^\dagger_{\mathbf{k},j}\hat{a}_{\mathbf{k},j} - \frac{q}{m_0 c}\hat{\mathbf{p}}\cdot\hat{\mathbf{A}}(\mathbf{r}(t)) + \frac{q}{2m_0^3 c^3}\hat{\mathbf{p}}^2\hat{\mathbf{p}}\cdot\hat{\mathbf{A}}(\mathbf{r}(t)). \tag{B4}$$

The interaction Hamiltonian in the interaction picture is

$$\hat{H}^I = \int d\mathbf{p}|\mathbf{p}\rangle\langle\mathbf{p}| \otimes \left(-\frac{q}{m_0 c} + \frac{q}{2m_0^3 c^3}\mathbf{p}^2\right)\mathbf{p}\cdot\hat{\mathbf{A}}(\mathbf{r}(t)). \tag{B5}$$

Therefore, the evolution operator can be written as

$$\hat{U}^I_{S:F}(t) = \int d^3 p|\mathbf{p}\rangle\langle\mathbf{p}| \otimes \hat{U}^I_F(t;\mathbf{p}), \tag{B6}$$

where

$$\hat{U}^I_F(t;\mathbf{p}) \equiv e^{i\sum_{\mathbf{k},j} C_{\mathbf{k}}\left(-1+\frac{1}{2m_0^2 c^2}\mathbf{p}^2\right)\mathbf{p}\cdot\boldsymbol{\epsilon}_{\mathbf{k},j}\xi_{\mathbf{k}}(t)} \times \hat{D}\left(\left(-1+\frac{1}{2m_0^2 c^2}\mathbf{p}^2\right)\sum_{\mathbf{k},j} C_{\mathbf{k}}\mathbf{p}\cdot\boldsymbol{\epsilon}_{\mathbf{k},j}\alpha_{\mathbf{k}}(t)\right). \tag{B7}$$

Repeating calculations of the previous section we find

$$-\Gamma^{(2)}_{\mathbf{p},\mathbf{p}'}(t) = \frac{1}{2}\sum_{\mathbf{k}_{\rm unob},j}|C_{\mathbf{k}}\alpha_{\mathbf{k}}(t)|^2\left|\left[\Delta\mathbf{p} + \frac{\mathbf{p}^2\mathbf{p} - \mathbf{p}'^2\mathbf{p}'}{2m_0^2 c^2}\right]\cdot\boldsymbol{\epsilon}_{\mathbf{k},j}\right|^2 \times \coth\left(\frac{\beta\omega_k}{2}\right). \tag{B8}$$

Proceeding as previously one arrives at

$$-\Gamma^{(2)}_{\mathbf{p},\mathbf{p}'}(t) = -\Gamma^{(1)}_{\mathbf{p},\mathbf{p}'}(t) + \frac{\alpha/\pi}{(m_0 c)^4}\left(I_1^{\rm vac}+I_1^{\rm th}\right) \times \int_{\Omega_{\rm unob}}\frac{d\Omega_{\mathbf{k}}}{4\pi}\sum_j(\Delta\mathbf{p}\cdot\boldsymbol{\epsilon}_{\mathbf{k},j})[(\mathbf{p}^2\mathbf{p}-\mathbf{p}'^2\mathbf{p}')\cdot\boldsymbol{\epsilon}_{\mathbf{k},j}] + \frac{v_0^2}{c^2}\frac{\alpha/\pi}{(m_0 c)^2}\left[2\left(I_1^{\rm vac}+I_1^{\rm th}\right) - 2t\left(I_2^{\rm vac}+I_2^{\rm th}\right) + t^2\left(I_3^{\rm vac}+I_3^{\rm th}\right)\right]\int_{\Omega_{unob}}\frac{d\Omega_{\mathbf{k}}}{4\pi}\cos^2\theta_{\mathbf{k}}\Delta\mathbf{p}^2_{\perp\mathbf{k}}, \tag{B9}$$

where

$$\int_0^\infty d\omega e^{-\frac{\omega}{\Omega}}\coth\left(\frac{\beta\omega}{2}\right)\omega\cos(\omega t) = I_3^{\rm vac} + I_3^{\rm th},$$

$$I_3^{\rm vac} \equiv \int_0^\infty d\omega e^{-\frac{\omega}{\Omega}}\omega\cos(\omega t),$$

$$I_3^{\rm th} \equiv \int_0^\infty d\omega e^{-\frac{\omega}{\Omega}}\left[\coth\left(\frac{\beta\omega}{2}\right)-1\right]\omega\cos(\omega t). \tag{B10}$$

The only change in calculation concerning fidelity will be that, starting from Eq. (B8) hyperbolic cotangent will be replaced by hyperbolic tangent. This will result in different frequency integrals but will not change the conclusion regarding relativistic terms obtained in Eq. (B9).

Hence we see that the logarithm of the decoherence factor and fidelity is formally of fourth order in $1/c$ and is thus two orders higher than the Hamiltonian (B4). This is a general characteristic of this calculation: The effect will be formally two orders higher than the Hamiltonian. The root of this lies simply in the passage to the continuum limit and the use of the dispersion relation.

[1] L. Landau, Z. Phys. **45**, 430 (1927).
[2] N. Bohr and L. Rosenfeld, K. Danske Vidensk. Selsk, Math.-Fys. Medd. **XII**, 8 (1933).
[3] M. Horodecki and J. Oppenheim, Nat. Commun. **4**, 2059 (2013).
[4] W. H. Zurek, Nat. Phys. **5**, 181 (2009).
[5] M. A. Schlosshauer, *Decoherence and the Quantum-to-Classical Transition* (Springer, Berlin, 2007).
[6] W. H. Zurek, Phys. Today **67**(10), 44 (2014).
[7] P. Skrzypczyk, A. J. Short, and S. Popescu, Nat. Commun. **5**, 4185 (2014).
[8] F. G. S. L. Brandão, M. Horodecki, N. H. Y. Ng, J. Oppenheim, and S. Wehner, Proc. Natl. Acad. Sci. USA **112**, 3275 (2015).
[9] H.-P. Breuer and F. Petruccione, *The Theory of Open Quantum Systems* (Oxford University Press, Oxford, 2002).
[10] E. Joos, H. D. Zeh, C. Kiefer, D. Guilini, J. Kupsch, and I.-O. Stamatescu, *Decoherence and the Appearance of a Classical World in Quantum Theory* (Springer, Berlin, 2003).
[11] H.-P. Breuer and F. Petruccione, Phys. Rev. A **63**, 032102 (2001).
[12] B. Bellomo, G. Compagno, and F. Petruccione, Phys. Rev. A **74**, 052112 (2006).
[13] M. A. Schlosshauer, in *Compendium of Quantum Physics*, edited by D. Greenberger, K. Hentschel, and F. Weinert (Springer, Berlin, 2009).
[14] J. K. Korbicz, P. Horodecki, and R. Horodecki, Phys. Rev. Lett. **112**, 120402 (2014).
[15] R. Horodecki, J. K. Korbicz, and P. Horodecki, Phys. Rev. A **91**, 032122 (2015).
[16] J. Tuziemski and J. K. Korbicz, Europhys. Lett. **112**, 40008 (2015).
[17] J. Tuziemski and J. Korbicz, Photonics **2**, 228 (2015).
[18] F. G. S. L. Brandão, M. Piani, and P. Horodecki, Nat. Commun. **6**, 7908 (2015).
[19] J. J. Sakurai, *Advanced Quantum Mechanics* (Addison-Wesley, Reading, MA, 1967).
[20] M. Zwolak, H. T. Quan, and W. H. Zurek, Phys. Rev. Lett. **103**, 110402 (2009).
[21] M. Zwolak, H. T. Quan, and W. H. Zurek, Phys. Rev. A **81**, 062110 (2010).
[22] M. Zwolak, C. J. Riedel, and W. H. Zurek, Phys. Rev. Lett. **112**, 140406 (2014).
[23] C. A. Fuchs and J. van de Graaf, IEEE Trans. Inf. Theory **45**, 1216 (1999).
[24] State fidelity is the same in the interaction and Schrödinger pictures.
[25] W. H. Zurek, in *Science and Ultimate Reality: Quantum Theory, Cosmology, and Complexity*, edited by J. D. Barrow, P. C. W. Davies, and C. L. Harper (Cambridge University Press, Cambridge, 2004).
[26] J. Dziarmaga, D. A. R. Dalvit, and W. H. Zurek, Phys. Rev. A **69**, 022109 (2004).
[27] C. J. Riedel and W. H. Zurek, Phys. Rev. Lett. **105**, 020404 (2010).
[28] C. J. Riedel and W. H. Zurek, New J. Phys. **13**, 073038 (2011).
[29] This is similar to the description of fluids: One considers portions of the fluid which macroscopically can be viewed as points but microscopically still contain a large enough amount of particles to define, e.g., the temperature.
[30] In the context of information extraction, the introduction of the cutoff in Eq. (22) may be given a natural interpretation of the maximum bandwidth of the detectors.
[31] M. Piani, P. Horodecki, and R. Horodecki, Phys. Rev. Lett. **100**, 090502 (2008).
[32] J. K. Korbicz, P. Horodecki, and R. Horodecki, Phys. Rev. A **86**, 042319 (2012).
[33] M. Zwolak and W. H. Zurek, Sci. Rep. **3**, 1729 (2013).
[34] C. J. Riedel, W. H. Zurek, and M. Zwolak, New J. Phys. **14**, 083010 (2012).
[35] The appearance of a limit on the momentum discrimination accuracy (26) connects with a concept of macroscopic objectivity, introduced in [17]: For sufficiently coarse-grained momenta they appear as objective, while this breaks at smaller scales.
[36] E. Joos and H. D. Zeh, Z. Phys. B Con. Mat. **59**, 223 (1985).
[37] I. Białynicki-Birula and T. Sowiński, Phys. Rev. A **76**, 062106 (2007).
[38] A. Lampo, J. Tuziemski, M. Lewenstein, and J. K. Korbicz, Phys. Rev. A **96**, 012120 (2017).
[39] F. Galve, R. Zambrini, and S. Maniscalco, Sci. Rep. **6**, 19607 (2016).